New Intermetallic Zinc Compounds with Ordering Variants of the KHg_2 and LT-$SrZn_5$ Type

Christian Schwickert and Rainer Pöttgen

Institut für Anorganische und Analytische Chemie, Universität Münster, Corrensstrasse 30, 48149 Münster, Germany

Reprint requests to R. Pöttgen. E-mail: pottgen@uni-muenster.de

Z. Naturforsch. **2014**, *69b*, 674 – 680 / DOI: 10.5560/ZNB.2014-4030
Received February 17, 2014

The intermetallic zinc compounds CaAuZn, SrPdZn, SrPtZn, SrAuZn, $BaPd_{1.57}Zn_{3.43}$, and $BaAu_{1.41}Zn_{3.59}$ were synthesized from the elements in sealed niobium ampoules in an induction furnace. The equiatomic compounds crystallize with the orthorhombic TiNiSi-type structure, space group *Pnma*. Single-crystal X-ray data exhibited small degrees of Au/Zn mixing within the three-dimensional [AuZn] networks and resulted in the compositions $CaAu_{1.02}Zn_{0.98}$ and $SrAu_{1.03}Zn_{0.97}$ for two investigated single crystals. $BaPd_{1.57}Zn_{3.43}$ and $BaAu_{1.41}Zn_{3.59}$ adopt partially ordered versions of the LT-$SrZn_5$ type, space group *Pnma*. Both structures were refined on the basis of X-ray single-crystal diffractometer data: $a = 1331.13(6)$, $b = 531.45(3)$, $c = 682.20(4)$ pm, $wR = 0.0245$, 1138 F^2 values, 39 variables for $BaPd_{1.57}Zn_{3.43}$ and $a = 1344.35(2)$, $b = 537.47(2)$, $c = 691.22(4)$ pm, $wR = 0.0441$, 931 F^2 values, 37 refined variables for $BaAu_{1.41}Zn_{3.59}$. The transition metal and zinc atoms form a complex three-dimensional network of $(T, Zn)_4$ tetrahedra which are condensed *via* common corners and *T*/Zn–*T*/Zn bonds. Large cavities within these networks are filled by the barium atoms which have coordination number 19, *i. e.* $Ba@(T, Zn)_{17}Ba_2$.

Key words: Zinc, Alkaline Earth Compounds, TiNiSi Type, LT-$SrZn_5$ Type

Introduction

In the structural chemistry of intermetallic compounds magnesium plays an interesting role in that it does not behave like the heavier alkaline earth elements; a situation similar to beryllium. In ternary systems *RE*-*T*-Mg and *AE*-*T*-Mg (*RE* = rare earth element; *AE* = alkaline earth element) one observes incorporation of the magnesium atoms into the two- or three-dimensional $[T_xMg_y]^{\delta-}$ polyanionic networks, emphasizing the covalent nature of magnesium within these compounds [1, 2]. Especially the alkaline earth compounds show clear segregation of magnesium from the heavier congeners. Recent examples are the compounds $SrPdMg_2$ [3] with a lonsdaleite-related magnesium substructure, CaPdMg with a three-dimensional $[PdMg]^{\delta-}$ polyanionic network [4] and $Ca_4Ag_{0.948}Mg$ with isolated Mg_4 tetrahedra [5]. Cadmium shows very similar crystal chemical behavior, and meanwhile many isotypic compounds have been reported [6].

Keeping the remarkable magnesium and cadmium substructures especially in the calcium, strontium and barium compounds in mind, we started further investigations with zinc. So far only few examples are known, *i. e.* the solid solution $BaAu_xZn_{13-x}$ with $NaZn_{13}$ superstructure variants [7], $CaNi_2Zn_3$ with an ordered $CaCu_5$ structure, CaAgZn with the KHg_2-type structure [8], and the TiNiSi-type $CaPd_{0.85}Zn_{1.15}$, complemented by the complex structures of $Ca_{21}Ni_2Zn_{36}$ and $Ca_6Pt_3Zn_5$ [9], $CaAu_4Zn_2$ with zinc chains [10], and $Sr_2Au_6Zn_3$ with Zn_3 triangles [11].

In continuation of the phase-analytical work we have now obtained the new zinc compounds CaAuZn, SrPdZn, SrPtZn, and SrAuZn with TiNiSi type, as well as $BaPd_{1.57}Zn_{3.43}$ and $BaAu_{1.41}Zn_{3.59}$ with ordered LT-$SrZn_5$ type. The synthesis and crystal chemical data of these phases are reported herein.

Experimental

Synthesis

Starting materials for the preparation of the *AETZn* (*AE* = Ca, Sr; *T* = Pd, Pt, Au) and $BaT_{2-x}Zn_{3+x}$ samples were calcium rods (Alfa Aesar, 99.5 %), strontium rods

(Johnson Matthey, > 99.9 %), barium rods (Alfa Aesar, > 99 %), snips of a palladium plate (Allgussa AG, 99.9 %), platinum sponge (Degussa-Hüls, > 99.9 %), gold ingots (Heraeus, > 99.9 %), and zinc granules (Merck, > 99.9 %). Suitable pieces of the alkaline earth metals were cleaned from surface impurities under dry paraffin oil, washed with cyclohexane and kept in Schlenk tubes under argon prior to the reactions. The *AET*Zn compounds were prepared by weighing the elements in the ideal equiatomic ratios and arc-welding them [12] in niobium ampoules with reduced argon pressure (purified over titanium sponge (900 K), silica gel and molecular sieves) of *ca.* 700 mbar. The sealed tubes were then placed inside evacuated silica ampoules and reacted in resistance furnaces. They were heated to 1300 K within two hours, kept at that temperature for another two hours and then slowly cooled to 950 K within ten hours, followed by 96 h of annealing. The resulting cast samples exhibit silvery luster while ground powders appear light grey.

Single crystals of $BaAu_{1.41}Zn_{3.59}$ and $BaPd_{1.57}Zn_{3.43}$ were first obtained when searching for equiatomic barium analogs of SrAuZn and SrPdZn. Subsequently bulk samples with starting compositions Ba : 1.6Pd : 3.4Zn and Ba : 1.4Au : 3.6Zn were weighted in the ideal stoichiometric ratios and arc-welded in niobium ampoules (*vide supra*). They were then placed in a water-cooled sample chamber of an induction furnace [13] (Typ TIG 2.5/300, Hüttinger Elektronik, Freiburg, Germany) and slowly heated to 1400 K under flowing argon. After ten minutes the temperature was slowly reduced to 800 K within 30 minutes, and the samples were annealed for 4 h. The polycrystalline samples exhibit silvery luster, and ground powders are medium grey. No reaction with the container material was observed for any of the synthesized compounds, but they show slow decomposition in air over months.

EDX data

The single crystals selected for intensity data collection on the diffractometers and the bulk samples were analyzed using a Zeiss EVO® MA10 scanning electron microscope with CaF_2, BaF_2, SrF_2, Pd, Pt, Au, and Zn as standards for the semiquantitative EDX analysis. No impurity elements heavier than Na (detection limit of the instrument) were observed. Especially no contaminations with the container material niobium were evident. The irregular surface of the samples (conchoidal fracture) hampered quantitative analyses.

X-Ray diffraction

Guinier powder patterns (Fujifilm image plate system, BAS-1800) were recorded for all polycrystalline samples using Cu$K\alpha_1$ radiation and α-quartz ($a = 491.30$, $c = 540.46$ pm) as an internal standard. The orthorhombic lattice parameters (Table 1) were obtained from least-squares refinements. Correct indexing of the patterns was ensured by intensity calculations [14]. The powder lattice parameters showed reasonable agreement with the single crystal data (Tables 1 and 2). The deviations observed for the barium compounds are a consequence of the homogeneity range.

Irregularly shaped crystals were obtained by mechanical fragmentation of the ingots. They were glued to quartz fibers using beeswax, immersed in superglue for hydrolysis/oxidation protection and investigated by Laue photographs on a Buerger camera (white molybdenum radiation, Fujifilm image plate technique, BAS-1800) in order to check their quality for intensity data collection. The $CaAu_{1.02}Zn_{0.98}$ crystal was measured at room temperature by use of a Stoe StadiVari (Mo microfocus source, Pilatus 100 K Detector) while the intensity data sets for $SrAu_{1.03}Zn_{0.97}$, $BaPd_{1.57}Zn_{3.43}$ and $BaAu_{1.41}Zn_{3.59}$ were obtained with a Stoe IPDS-II image plate system (graphite-monochromatized Mo radiation; $\lambda = 71.073$ pm, oscillation

Table 1. Orthorhombic lattice parameters (Guinier powder data) of the TiNiSi-type compounds *RT*Zn and the LT-$SrZn_5$-type compounds $BaPd_{1.8}Zn_{3.2}$ and $BaAu_{1.4}Zn_{3.6}$.

Compound	a (pm)	b (pm)	c (pm)	V (nm^3)	Reference
YbPdZn	699.7(1)	423.2(1)	794.2(1)	0.2352	[26]
$CaPd_{0.85}Zn_{1.15}$	717.28(9)	439.49(5)	774.30(9)	0.2441	[9]
EuPdZn	732.3(2)	448.5(2)	787.7(2)	0.2587	[15]
SrPdZn	746.3(3)	453.7(2)	787.6(4)	0.2666	this work
YbPtZn	684.2(1)	405.7(1)	810.3(1)	0.2249	[26]
EuPtZn	727.8(3)	443.7(1)	781.7(3)	0.2524	[15]
SrPtZn	740.7(3)	448.9(4)	781.8(5)	0.2599	this work
YbAuZn	713.5(1)	445.6(1)	789.8(1)	0.2511	[26]
CaAuZn	723.9(2)	448.9(1)	784.9(2)	0.2549	this work
EuAuZn	747.4(2)	465.8(2)	789.1(4)	0.2747	[15]
SrAuZn	767.6(3)	468.2(3)	801.9(4)	0.2882	this work
$BaPd_{1.8}Zn_{3.2}$	1325.5(6)	529.3(3)	676.7(3)	0.4793	this work
$BaAu_{1.4}Zn_{3.6}$	1347.1(4)	541.4(2)	689.2(2)	0.5026	this work

Table 2. Crystal data and structure refinement for $CaAu_{1.02}Zn_{0.98}$, $SrAu_{1.03}Zn_{0.97}$, $BaPd_{1.57}Zn_{3.43}$, and $BaAu_{1.41}Zn_{3.59}$, space groups *Pnma*, $Z = 4$, Mo$K\alpha$ (71.073 pm).

Empirical formula	$CaAu_{1.02}Zn_{0.98}$	$SrAu_{1.03}Zn_{0.97}$	$BaPd_{1.57}Zn_{3.43}$	$BaAu_{1.41}Zn_{3.59}$
Molar mass, g mol^{-1}	304.5	353.3	528.7	649.9
Unit cell dimensions (single crystal data)				
a, pm	724.39(4)	765.51(7)	1331.13(6)	1344.35(2)
b, pm	449.15(2)	465.92(4)	531.45(3)	537.47(2)
c, pm	784.98(5)	799.90(9)	682.20(4)	691.22(4)
V, nm^3	0.2554	0.2853	0.4826	0.4994
Calculated density, g cm^{-3}	7.92	8.22	7.27	8.64
Crystal size, μm^3	$40 \times 40 \times 60$	$50 \times 50 \times 70$	$9 \times 25 \times 55$	$7 \times 45 \times 65$
Diffractometer	Stoe StadiVari	Stoe IPDS-II	Stoe IPDS-II	Stoe IPDS-II
Transm. ratio (max/min)	0.346/0.164	0.438/0.121	0.589/0.236	0.204/0.044
Absorption coefficient, mm^{-1}	70.1	79.0	30.3	65.8
F(000), e	524	594	925	1099
θ range, deg	3 – 35	3 – 35	3 – 35	3 – 32
Range in *hkl*	±11, ±7, ±12	±12, ±7, ±12	±21, ±8, ±10	±19, ±7, ±10
Total no. reflections	11 150	7181	20 852	17 053
Independent reflections/R_{int}	614/0.0605	687/0.1059	1138/0.0720	931/0.0740
Reflections with $I > 3\sigma(I)/R_\sigma$	491/0.0230	580/0.0201	671/0.0373	879/0.0051
Data/parameters	614/21	687/21	1138/39	931/37
Goodness-of-fit on F^2	1.08	2.03	0.52	1.67
R/wR for $I > 3\sigma(I)$	0.0192/0.0424	0.0356/0.0732	0.0113/0.0200	0.0197/0.0432
R/wR for all data	0.0250/0.0431	0.0456/0.0749	0.0385/0.0245	0.0229/0.0441
Extinction coefficient	452(15)	2700(200)	1380(50)	3040(120)
Largest diff. peak/hole, e^{-3}	1.27/–1.43	4.55/–3.53	0.96/–1.01	1.70/–1.99

mode). Spherical (Stoe StadiVari) and numerical (Stoe IPDS-II) absorption corrections were applied to all data sets. Details of the data collections and the structure refinements are listed in Table 2.

Structure refinements

Analyses of the data sets for $CaAu_{1.02}Zn_{0.98}$, $SrAu_{1.03}Zn_{0.97}$, $BaPd_{1.57}Zn_{3.43}$, and $BaAu_{1.41}Zn_{3.59}$ revealed primitive orthorhombic lattices, and the systematic extinctions were in accordance with the space group *Pnma*. Isotypism of $CaAu_{1.02}Zn_{0.98}$ and $SrAu_{1.03}Zn_{0.97}$ with EuAuZn (TiNiSi type) was already evident from the Guinier powder patterns. The atomic parameters of EuAuZn [15] were taken as starting values, and the two structures were refined on F^2 with anisotropic displacement parameters for all atoms using the JANA2006 [16] routine. Since TiNiSi-type $CaPd_{0.85}Zn_{1.15}$ [9] and related equiatomic magnesium and

Table 3. Atomic positions and equivalent isotropic displacement parameters of $CaAu_{1.02}Zn_{0.98}$ and $SrAu_{1.03}Zn_{0.97}$ with TiNiSi-type structure as well as $BaPd_{1.57}Zn_{3.43}$ and $BaAu_{1.41}Zn_{3.59}$ with LT-SrZn_5-type structure, space groups *Pnma*, $Z = 4$.

Atom	Site	*x*	*y*	*z*	U_{eq}
$CaAu_{1.02}Zn_{0.98}$					
Ca	4*c*	0.0088(2)	1/4	0.6954(2)	206(3)
Au	4*c*	0.28722(4)	1/4	0.39983(4)	211(1)
0.98(1)Zn + 0.02(1)Au	4*c*	0.67020(13)	1/4	0.42364(10)	223(3)
$SrAu_{1.03}Zn_{0.97}$					
Sr	4*c*	0.00455(14)	1/4	0.70026(13)	138(3)
0.96(1)Au1 + 0.04(1)Zn1	4*c*	0.29691(6)	1/4	0.40815(6)	153(1)
0.93(1)Zn2 + 0.07(1)Au2	4*c*	0.68010(18)	1/4	0.41978(16)	176(4)
$BaPd_{1.57}Zn_{3.43}$					
Ba	4*c*	0.41446(2)	1/4	0.86551(3)	175(1)
0.95(1)Zn1 + 0.05(1)Pd1	4*c*	0.21184(4)	1/4	0.17046(5)	153(2)
0.79(1)Pd2 + 0.21(1)Zn2	4*c*	0.21521(3)	1/4	0.55615(4)	158(1)
0.92(1)Zn3 + 0.08(1)Pd3	8*d*	0.35532(2)	−0.00024(5)	0.35399(4)	135(1)
0.58(1)Pd4 + 0.42(1)Zn4	4*c*	0.02041(3)	1/4	0.08195(5)	155(1)
$BaAu_{1.41}Zn_{3.59}$					
Ba	4*c*	0.41543(3)	1/4	0.86459(5)	169(1)
Zn1	4*c*	0.21149(5)	1/4	0.17092(11)	161(2)
0.88(1)Au2 + 0.12(1)Zn2	4*c*	0.21209(2)	1/4	0.55750(3)	150(1)
Zn3	8*d*	0.35506(3)	0.00017(8)	0.35572(7)	138(1)
0.53(1)Au4 + 0.47(1)Zn4	4*c*	0.01931(2)	1/4	0.09158(5)	161(1)

cadmium compounds [2, 6, 17, 18] revealed small degrees of *T*-Zn, *T*-Mg, and *T*-Cd mixing, the gold and zinc occupancy parameters of both crystals were refined in separate series of least-squares cycles. These refinements revealed only a small degree of gold on the zinc site of $CaAu_{1.02}Zn_{0.98}$, while both sites showed mixed occupancy in $SrAu_{1.03}Zn_{0.97}$. In the final cycles these occupancies were refined as least-squares variables.

The initial atomic parameters for the two barium compounds were deduced using the charge-flipping algorithm of SUPERFLIP [19], and again the structures were refined on F^2 with anisotropic displacement parameters with JANA2006. The structure solution revealed the Pearson symbol *oP*24 with the Wyckoff sequence dc^4. Inspection of the Pearson data base [20] revealed isotypism with the low-temperature (LT) modification of $SrZn_5$ [21, 22]. The setting of LT-$SrZn_5$ [22] was then used for the subsequent cycles, and the respective Pd/Zn and Au/Zn mixed occupancies were refined as least-squares variables, leading to the compositions listed in Table 2. The final difference Fourier synthesis revealed no significant residual peaks. The final positional parameters and interatomic distances are listed in Tables 3 – 5.

Further details of the crystal structure investigations may be obtained from Fachinformationszentrum Karlsruhe, 76344 Eggenstein-Leopoldshafen, Germany (fax: +49-7247-808-666; e-mail: crysdata@fiz-karlsruhe.de, http://www.fiz-karlsruhe.de/request_for_deposited_data.html) on quoting the deposition numbers CSD-427365 ($CaAu_{1.02}Zn_{0.98}$), CSD-427366 ($SrAu_{1.03}Zn_{0.97}$), CSD-427367 ($BaPd_{1.57}Zn_{3.43}$), and CSD-427368 ($BaAu_{1.41}Zn_{3.59}$).

Table 4. Interatomic distances (pm, calculated with the powder lattice parameters) in the structure of $CaAu_{1.02}Zn_{0.98}$. Standard deviations are all equal to or smaller than 0.2 pm. All distances within the first coordination spheres are listed. Note the small degree of Zn/Au mixing (Table 3).

Ca:	1	Au	307.4	Au:	2	Zn	265.7
	2	Au	313.1		1	Zn	267.7
	2	Zn	315.2		1	Zn	278.1
	2	Au	319.4		1	Ca	307.4
	1	Zn	321.1		2	Ca	313.1
	1	Zn	325.1		2	Ca	319.4
	2	Zn	336.5		1	Ca	356.0
	1	Au	356.0	Zn:	2	Au	265.7
	2	Ca	372.2		1	Au	267.7
	2	Ca	380.4		1	Au	278.1
					2	Ca	315.2
					1	Ca	321.1
					1	Ca	325.1
					2	Ca	336.5

Discussion

Phase-analytical work in the *AE*-*T*-Zn systems revealed the new intermetallic compounds CaAuZn, SrPdZn, SrPtZn, SrAuZn, $BaPd_{1.57}Zn_{3.43}$, and $BaAu_{1.41}Zn_{3.59}$. All compounds show small homogene-

Table 5. Interatomic distances (pm) in the structure of $BaAu_{1.41}Zn_{3.59}$. Standard deviations are all equal to or smaller than 0.1 pm. All distances within the first coordination spheres are listed.

Ba:	2	Au4/Zn4	339.9	Zn3:	1	Au4/Zn4	261.0
	1	Au4/Zn4	344.9		1	Au2/Zn2	262.1
	2	Zn1	345.3		1	Zn1	267.6
	2	Au2/Zn2	345.5		1	Zn3	268.6
	1	Au2/Zn2	346.1		1	Zn3	268.9
	1	Zn1	346.4		1	Au4/Zn4	270.5
	2	Zn3	369.4		1	Zn1	271.2
	2	Zn3	374.0		1	Au2/Zn2	272.8
	2	Zn3	385.1		1	Ba	369.4
	2	Zn3	387.7		1	Ba	374.0
	2	Ba	398.7		1	Ba	385.1
Zn1:	1	Au4/Zn4	264.1		1	Ba	387.7
	1	Au2/Zn2	267.2	Au4/Zn4:	2	Zn3	261.0
	2	Zn3	267.6		1	Zn1	264.1
	2	Zn3	271.2		2	Zn3	270.5
	2	Au2/Zn2	298.2		2	Au4/Zn4	301.6
	2	Ba	345.3		2	Ba	339.9
	1	Ba	346.4		1	Ba	344.9
Au2/Zn2:	2	Zn3	262.1				
	1	Zn1	267.2				
	2	Zn3	272.8				
	2	Zn1	298.2				
	2	Ba	345.5				
	1	Ba	346.1				

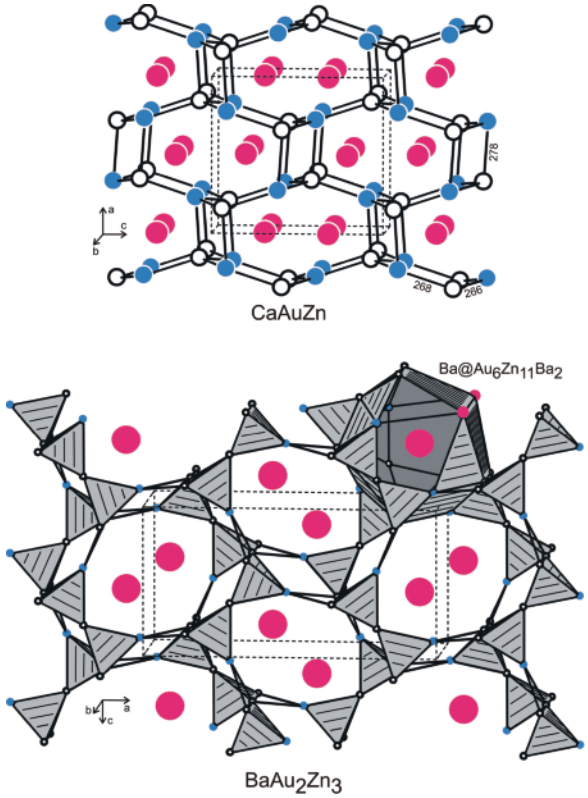

Fig. 1. (color online). The crystal structures of CaAuZn (TiNiSi type, *Pnma*) and $BaAu_2Zn_3$ (LT-$SrZn_5$ type, *Pnma*). Alkaline earth, gold and zinc atoms are drawn as red, blue and black open circles, respectively. The three-dimensional [AuZn] polyanionic network of CaAuZn is emphasized, and relevant interatomic distances are given. For $BaAu_2Zn_3$ (the two mixed occupied sites were drawn as pure gold sites) the network of condensed (Au, Zn)$_4$ tetrahedra is drawn along with one $Ba@Au_6Zn_{11}Ba_2$ polyhedron.

ity ranges due to transition metal-zinc mixing. The structures are derived from binary alkaline earth-zinc compounds through ordered occupancies on different Wyckoff sites.

Similar to $CaPd_{0.85}Zn_{1.15}$ [8], also CaAuZn, SrPdZn, SrPtZn and SrAuZn derive from KHg_2-type $CaZn_2$ [23] and $SrZn_2$ [24]. Exemplarily we discuss the CaAuZn structure herein. The difference in size between gold and zinc (the covalent radii [25] are 134 and 125 pm, respectively) lead to a distinct distortion of the zinc substructure. This leads to a decentering of the body-centered lattice of the KHg_2 type (space group *Imma*), and $CaAu_{1.02}Zn_{0.98}$ and $SrAu_{1.03}Zn_{0.97}$ adopt the TiNiSi-type structure, space group *Pnma* (*klassengleiche* subgroup of *Imma*) (Fig. 1).

The lattice parameters of the alkaline earth-based compounds are listed in Table 1 along with the isotypic intermetallics based on europium [15] and ytterbium [26]. In their [Xe]$4f^7$ and [Xe]$4f^{14}$ configuration Eu^{2+} and Yb^{2+} have radii comparable to those of Sr^{2+} and Ca^{2+}. From Table 1 it is evident that the cell volumes increase from the ytterbium to the strontium compounds. The by far smallest cell volume in this series occurs for YbPtZn [26]. This is caused by the presence of the smaller trivalent ytterbium atoms which was evident from the paramagnetic behavior along with magnetic ordering below 1.35 K. The TiNiSi-type structure shows large flexibility for the zinc compounds reported herein. While one observes an almost monotonic increase of the *a* and *b* parameters in the series of palladium, platinum and gold compounds in going from the ytterbium to the strontium member, the *c* parameter shows a minimum for the calcium compounds. In this way the structure is adjusted to the individual bond strength just by variation of the lattice parameters. The positional parameters show no pronounced variations (Table 3 and [15]).

The near-neighbor coordinations are shown in Fig. 2, viewed approximately along the *b* axis. These drawings nicely show the relationship with the aristotype AlB_2. The gold and zinc atoms build up corrugated layers of ordered Au_3Zn_3 hexagons with Au–Zn distances ranging from 265 to 277 pm, slightly longer than the sum of the covalent radii of 259 pm for Au + Zn [25]. The different degrees of puckering result in different Au-Zn-Au angles within the Au_2Zn_2 rhombs. The latter ones are formed as a result of the inter-layer Au–Zn bonding. These Au–Zn distances of 274 – 294 pm are significantly longer than the intra-layer Au–Zn distances. Within the Au_2Zn_2 rhombs, the gold atoms as the most electronegative components show maximal separation. This is a general trend in TiNiSi-related structures [27, 28].

A view of the CaAuZn structure approximately along the *b* axis is presented in Fig. 1. Due to the strong puckering of the honeycomb network, the gold and zinc atoms both show strongly distorted tetrahedral $AuZn_{4/4}$, respectively $ZnAu_{4/4}$ coordination. The calcium atoms bind to the [AuZn] network *via* the gold atoms. The three closest gold

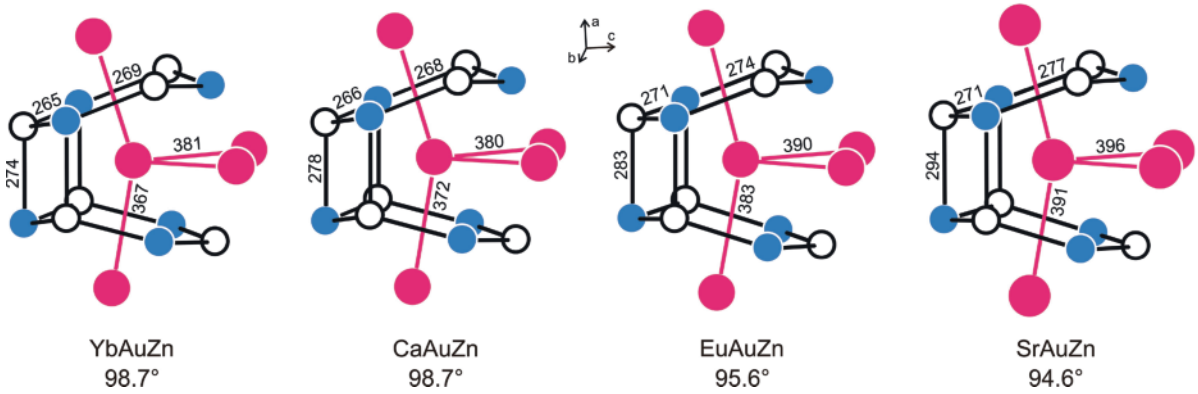

Fig. 2. (color online). Coordination of the ytterbium, calcium, europium, and strontium atoms in YbAuZn, CaAuZn, EuAuZn, and SrAuZn. Gold and zinc atoms are drawn as blue and black open circles, respectively. Relevant interatomic distances and the Au–Zn–Au angles within the Au_2Zn_2 rhombs are given. For YbAuZn we used the positional parameters of CaAuZn.

neighbors are at Ca–Au distances in the range of 307 to 313 pm, similar to the structures of Ca_3Au_3In (300 – 315 pm) [29], $CaAu_4Cd_2$ (306 pm) [30] and $CaAu_4Zn_2$ (295 pm) [10]. Keeping the course of the electronegativities in mind, one can ascribe auride character to both CaAuZn and SrAuZn. Nevertheless we keep the element sequence in the formulæ for better comparison with the isotypic compounds. For further crystal chemical details on TiNiSi-type intermetallics we refer to a review article [31].

The ternary compounds $BaPd_{1.57}Zn_{3.43}$ and $BaAu_{1.41}Zn_{3.59}$ are also derived from a binary structure type. They can be considered as ordering variants of the LT-$SrZn_5$ type [21, 22]. While all four zinc sites show mixed occupancy in the palladium compound, only two sites exhibit Au/Zn mixing in $BaAu_{1.41}Zn_{3.59}$ (Table 3). Fully ordered variants have recently been observed for the gallides $RbAu_3Ga_2$ and $CsAu_3Ga_2$ [32]. As an example for the zinc compounds we discuss the $BaAu_{1.41}Zn_{3.59}$ structure herein. Binary $BaZn_5$ crystallizes with its own structure type (space group *Cmcm*) and shows no dimorphism. Addition of palladium or gold leads to a switch in structure type towards LT-$SrZn_5$. The only ternary ordered variant for the $BaZn_5$ type is KAu_3Ga_2 [33]. The crystal-chemical relationship between the $BaZn_5$ and LT-$SrZn_5$ structures is discussed in detail in [21, 22].

A view of the $BaAu_{1.41}Zn_{3.59}$ structure approximately along the *b* axis is presented in Fig. 1 (the two mixed-occupied sites were drawn as pure gold sites). Similar to the CaAuZn structure discussed above, we observe the shortest interatomic distances between the gold and zinc atoms. The Au–Zn distances range from 261 to 298 pm, a slightly broader range than observed for CaAuZn. Again, the gold and zinc atoms build up a three-dimensional network which is composed of $(Au/Zn)_4$ tetrahedra which are condensed *via* two common corners, and further *via* Au–Zn bonds. This network leaves large cavities which are filled by the barium atoms with a coordination of Ba@$(Au, Zn)_{17}Ba_2$. The triangular faces of this coordination polyhedron derive from the $(Au/Zn)_4$ tetrahedra. The shortest Ba–Ba distance between two adjacent barium atoms is 399 pm (an edge of each Ba@$(Au, Zn)_{17}Ba_2$ polyhedron), somewhat shorter than the Ba–Ba distance of 435 pm for the eight nearest neighbors in *bcc* barium [34]. However, in view of the strongly differing Pauling electronegativities (0.89 for Ba, 2.54 for Au, 1.65 for Zn), one can assume a highly ionic character (and thus smaller size) of barium, and the interactions may not be considered as bonding. A similar situation occurs in many ternary lithium-based intermetallics [35, 36].

Besides substantial Au–Zn bonding one also observes a small range of Zn–Zn distances (268 – 271 pm) within the $[Au_{1.41}Zn_{3.59}]$ network. These Zn–Zn distances compare well with the shorter ones in *hcp* zinc (6×266 and 6×291 pm) [34]. Furthermore the Au4/Zn4–Au4/Zn4 distance of 302 pm is indicative of weak Au–Au bonding in those domains were only gold atoms occupy this position.

In summary, the new compounds reported herein mean a significant extension of the family of alkaline earth-transition metal-zinc intermetallics. Includ-

ing the few examples mentioned in the introduction, one can expect many more phases in the respective ternary systems, also including the other not yet tested electron-rich transition metals. More detailed phase-analytical studies are in progress.

Acknowledgement

We thank Dipl.-Ing. U. Ch. Rodewald for the intensity data collections. This work was financially supported by the Deutsche Forschungsgemeinschaft.

[1] R. Pöttgen, R.-D. Hoffmann, *Metall* **2004**, *58*, 557.
[2] U. Ch. Rodewald, B. Chevalier, R. Pöttgen, *J. Solid State Chem.* **2007**, *180*, 1720.
[3] M. Kersting, M. Johnscher, S. F. Matar, R. Pöttgen, *Z. Anorg. Allg. Chem.* **2013**, *639*, 707.
[4] M. Kersting, M. Johnscher, R. Pöttgen, *Z. Kristallogr.* **2013**, *228*, 635.
[5] M. Kersting, S. F. Matar, C. Schwickert, R. Pöttgen, *Z. Naturforsch.* **2012**, *67b*, 61.
[6] F. Tappe, R. Pöttgen, *Rev. Inorg. Chem.* **2011**, *31*, 5.
[7] S. Gupta, J. D. Corbett, *Inorg. Chem.* **2012**, *51*, 2247.
[8] M. Pani, M. L. Fornasini, F. Merlo, *Z. Kristallogr.* **2007**, *222*, 218.
[9] M. Stojanovic, S. E. Latturner, *J. Solid State Chem.* **2007**, *180*, 907.
[10] B. Gerke, O. Niehaus, R.-D. Hoffmann, R. Pöttgen, *Z. Anorg. Allg. Chem.* **2013**, *639*, 2575.
[11] B. Gerke, R.-D. Hoffmann, R. Pöttgen, *Z. Anorg. Allg. Chem.* **2013**, *639*, 2444.
[12] R. Pöttgen, T. Gulden, A. Simon, *GIT Labor-Fachzeitschrift* **1999**, *43*, 133.
[13] D. Kußmann, R.-D. Hoffmann, R. Pöttgen, *Z. Anorg. Allg. Chem.* **1998**, *624*, 1727.
[14] K. Yvon, W. Jeitschko, E. Parthé, *J. Appl. Crystallogr.* **1977**, *10*, 73.
[15] T. Mishra, W. Hermes, T. Harmening, M. Eul, R. Pöttgen, *J. Solid State Chem.* **2009**, *182*, 2417.
[16] V. Petříček, M. Dušek, L. Palatinus, JANA2006, The Crystallographic Computing System, Institute of Physics, University of Prague, Prague (Czech Republic) **2006**.
[17] Th. Fickenscher, R. Pöttgen, *J. Solid State Chem.* **2001**, *161*, 67.
[18] Th. Fickenscher, R.-D. Hoffmann, R. Kraft, R. Pöttgen, *Z. Anorg. Allg. Chem.* **2002**, *628*, 667.
[19] L. Palatinus, G. Chapuis, *J. Appl. Crystallogr.* **2007**, *40*, 786.
[20] P. Villars, K. Cenzual, Pearson's Crystal Data: Crystal Structure Database for Inorganic Compounds (release 2013/14), ASM International®, Materials Park, Ohio (USA) **2013**.
[21] N. C. Baenziger, J. W. Conant, *Acta Crystallogr.* **1956**, *9*, 361.
[22] M. Wendorff, C. Röhr, *Z. Naturforsch.* **2007**, *62b*, 1549.
[23] G. E. R. Schulze, J. Wieting, *Z. Metallkd.* **1961**, *52*, 743.
[24] B. G. Bergman, P. J. Shlichta, *Acta Crystallogr.* **1964**, *17*, 65.
[25] J. Emsley, *The Elements*, Oxford University Press, Oxford (U. K.) **1999**.
[26] S. K. Dhar, R. Kulkarni, P. Manfrinetti, M. Pani, Y. Yonezawa, Y. Aoki, *Phys. Rev. B* **2007**, *76*, 054411.
[27] G. Nuspl, K. Polborn, J. Evers, G. A. Landrum, R. Hoffmann, *Inorg. Chem.* **1996**, *35*, 6922.
[28] G. A. Landrum, R. Hoffmann, J. Evers, H. Boysen, *Inorg. Chem.* **1998**, *37*, 5754.
[29] I. R. Muts, V. I. Zaremba, U. C. Rodewald, R. Pöttgen, *Z. Anorg. Allg. Chem.* **2008**, *634*, 56.
[30] F. Tappe, S. F. Matar, C. Schwickert, F. Winter, B. Gerke, R. Pöttgen, *Monatsh. Chem.* **2013**, *144*, 751.
[31] R.-D. Hoffmann, R. Pöttgen, *Z. Kristallogr.* **2001**, *216*, 127.
[32] V. Smetana, G. J. Miller, J. D. Corbett, *Inorg. Chem.* **2012**, *51*, 7711.
[33] V. Smetana, J. D. Corbett, G. J. Miller, *Inorg. Chem.* **2012**, *51*, 1695.
[34] J. Donohue, *The Structures of the Elements*, Wiley, New York **1974**.
[35] R. Pöttgen, T. Dinges, H. Eckert, P. Sreeraj, H.-D. Wiemhöfer, *Z. Phys. Chem.* **2010**, *224*, 1475.
[36] T. Dinges, R.-D. Hoffmann, L. van Wüllen, P. Henry, H. Eckert, R. Pöttgen, *J. Solid State Electrochem.* **2011**, *15*, 237.